Crucial Effect of Angular Flexibility on the Fracture Toughness and Nano-Ductility of Aluminosilicate Glasses

Mengyi Wang[1], Bu Wang[1], Tobias K. Bechgaard[2], John C. Mauro[3], Sylwester J. Rzoska[4], Michal Bockowski[4], Morten M. Smedskjaer[2], Mathieu Bauchy[1,*]

[1] *Physics of AmoRphous and Inorganic Solids Laboratory (PARISlab), University of California, Los Angeles, CA 90095, USA*

[2] *Department of Chemistry and Bioscience, Aalborg University, Aalborg 9220, Denmark*

[3] *Science and Technology Division, Corning Incorporated, Corning, New York 14831, USA*

[4] *Institute of High Pressure Physics, Polish Academy of Sciences, Warsaw 00-142, Poland*

** Corresponding author e-mail: bauchy@ucla.edu*

Abstract

Understanding and controlling materials' resistance to fracture is critical for various applications. However, the structural origin of toughness, brittleness, and ductility remains poorly understood. Here, based on the experimental testing and atomistic simulations of a series of aluminosilicate glasses with varying thermal and pressure histories, we investigate the role of structure in controlling fracture toughness at fixed composition. We show that fracture toughness decreases with density, but strongly depends on the details of the temperature and pressure histories of the glass. This behavior is found to arise from a loss of nano-ductility rather than a loss of cohesion. Finally, we demonstrate that the propensity for nano-ductility is primarily controlled by the extent of angular flexibility between the rigid polytopes of the network. Tuning the extent of nano-ductility in silicate glasses would permit the design of ultra-tough glasses.

Keywords: Molecular dynamics, annealing, pressure effect, micro-indentation, toughness, ductility.

1. Introduction

Despite recent advances in the development high performance glasses – like Corning® Gorilla® Glass [1–3], a scratch- and damage-resistant glass used on more than 4 billion smartphone and tablet screens – glass still breaks. Developing novel glasses featuring higher resistance to cracking while retaining transparency would greatly extend the range of applications of glasses, e.g., for fiber optics, flexible substrates, or protective screens in extreme conditions [4]. In turn, the use of glasses with improved mechanical properties would also permit the use of thinner material while achieving similar performances. This would reduce the weight of glass panels, which, in the case of car windshields, would result in significant gas savings. Although extrinsic treatments like compositing [5], inclusion of holes [6], or surface treatments [7] can enhance glass toughness, they often result in undesirable side effects like a loss of transparency [4]. Alternatively, the recent observation that glass can feature some ductility at the nanoscale despite being brittle at the macroscale [8–10] offers a new degree of freedom to improve the intrinsic toughness of glasses.

However, our ability to enhance the intrinsic resistance to fracture of glasses is presently limited by a lack of understanding in the influence of composition and atomic structure on strength, fracture toughness, and brittleness. In fact, this gap of knowledge has recently been identified as a "Grand Challenge" in glass science [11–13]. Understanding such linkages is complicated by the difficulty of precisely isolating the effects of composition, packing density, short-range, medium-range, and long-range order structure on toughness.

Here, we consider a series of glasses of similar composition with differing temperature and pressure histories to isolate the effect of *only* structure on fracture toughness, that is, the fact that temperature and pressure histories each impact the short- and medium-range structure differently allows us to isolate the relative influence of each scale on fracture toughness. In detail, by combining experimental indentation tests and atomistic molecular dynamics (MD) simulations, we show that thermal annealing and pressure quenching treatments both affect fracture toughness, but in a drastically different fashion. The detailed investigation of the differing structural modifications induced by varying temperature and pressure histories reveals that the degree of brittleness of glass fracture is primarily controlled by the short-range order structure and, specifically, the extent of inter-tetrahedral motion in the atomic network. This emphasizes the important role of angular flexibility in controlling glasses' resistance to fracture.

2. Experimental and computational methods

2.1. Sample preparation

The glass used herein is a commercial alkaline earth aluminosilicate glass, i.e., Corning Jade® glass with a patented composition given in Ref. [14] and a glass transition temperature T_g = 1055 K. Due to its high thermal and chemical stability, this glass is typically used for pSi liquid crystal display substrates. The glass was manufactured using the fusion draw process, which yields a high initial fictive temperature T_f = 1125 K. Such high initial T_f allows us to investigate a wide range of thermal histories through annealing. We also point out that the fusion draw process ensures a high level of homogeneity, which is required to meaningfully compare the subtle effects of varying thermal and pressure histories [15].

Glass sheets with dimensions of approximately 25 × 25 × 0.7 mm^3 were prepared, and subsequently (1) annealed for times t_a varying from 5 min to 88 h at a temperature T_a = 1034 K (0.98 T_g) or (2) isostatically compressed at T_g for 30 min at pressures P varying from 0.1 and 1.0 GPa. Annealing was performed by placing the samples in a furnace at the temperature T_a for a pre-determined annealing time, before rapidly quenching the glass. Isostatic compression was achieved using a nitrogen gas pressure chamber, as described in details in Ref. [16]. The resulting glass densities were determined using Archimedes' principle with water as the immersion medium. Each measurement of sample weight was repeated ten times.

2.2. Indentation fracture toughness

The indentation fracture toughness K_c of the samples were determined using a Vickers micro-indenter (Duramin 5, Struers A/S) at a load of 9.8 N. The indent diagonal a and length c of radial/median corner cracks were measured using optical microscopy. From the measured

value of a, Vickers hardness H_V was determined. To calculate the indentation fracture toughness K_c, Young's modulus E is also required, which was determined based on measured sound velocities (ultrasonic pulse-echo technique) and densities. K_c was then subsequently determined by measuring the crack-to-indent size (c/a) ratio (see details in Ref. [17]). The measured c/a ratio was larger than 2.5 for all investigated samples, thus satisfying the condition of a semi-elliptical median-radial crack system and enabling K_c to be calculated based on the equation given in Refs. [18,19]. We note that the fracture toughness values obtained through Vickers indentation differ from those determined using other standardized tests [20], and can therefore only be used for relative internal comparisons. Nevertheless, determining fracture toughness using standard techniques like chevron notch beam (CNB) or V-notched beam (SEVNB) requires larger quantities of each sample, which, in the present case, were not available due to the limited volume of the utilized pressure vessel. As such, we rely here on Vickers indentation to determine the relative effects of varying thermal and pressure histories on fracture toughness, but remain fully aware that the results will not be quantitatively comparable to those obtained using the above-mentioned CNB or SEVNB techniques.

2.3. Molecular dynamics simulations

To gain deeper insights into the experimental trends observed herein, a $30CaO–10Al_2O_3–60SiO_2$ glass (in mol %) of 2995 atoms was simulated through classical MD. This composition was chosen to be similar – in terms of types and ratio of the major oxides – to that of the experimental glass, while remaining simple enough to be well documented, which is a necessary condition to validate the outcomes of the simulations. Note that, as the exact composition of the simulated glass differs from that of the glass synthesized herein, we do not expect an absolute agreement between simulations and experiments. Nevertheless, as shown below and in Ref. [21], the experimental and simulated glasses show similar trends in density, hardness, fracture toughness, and brittleness and, as such, can be compared on a relative basis. For this study, we relied on a two-body Born-Mayer-Huggins potential, recently parameterized by Jakse [22]. The details of the simulation parameters, as well as multiple structural, mechanical, and vibrational validations can be found in Refs. [9,23]. It is worth noting that the Jakse potential used herein was shown to offer the best agreement with available experimental structural data, as compared to various alternative potentials [23]. Note that the ability of the potential to predict a realistic structure is of primary importance here as we aim to understand the structural origin of toughness and brittleness. In particular, this potential was found to yield the best prediction of the Si–O–Si angle, with an improved level of agreement as compared to an alternative 3-body potential [23].

Following the synthesis protocol, the simulated systems were subsequently quenched under pressure or thermally annealed. As a starting configuration, a liquid was relaxed at 5000 K and zero pressure in the *NPT* ensemble for 1 ns. First, to study the effect of quenching under pressure only, i.e., without any annealing, several glasses were prepared by compressing during 1 ns the liquid in the *NPT* ensemble at 5000 K under a pressure varying from 0.5 to 2.5 GPa. Such duration was found to be long enough to ensure a full relaxation of the melt. The samples were then subjected to an instantaneous quenching down to 300 K. Each glass was eventually relaxed for 1 ns in the *NPT* ensemble at zero pressure. Second, to study the effect of annealing

only, the liquid was instantly quenched down to 1500 K, a temperature that is slightly lower than the simulated T_g. The system was then annealed in the *NPT* ensemble at 1500 K and zero pressure, with intermediate configurations being saved after 0 ps ("as-prepared" glass), 1 ps, 10 ps, and 1 ns of annealing. Each configuration was then instantly quenched down to 300 K and relaxed in the *NPT* ensemble at zero pressure for 1 ns. Finally, all systems were further sampled in the *NVT* ensemble at 300 K during 200 ps for statistical averaging. Pair distribution functions, interatomic distances, neutron structure factors, and angular distributions were computed and can be found in Refs. [21,23].

It is worth pointing out that, upon annealing, samples exchange heat through their surfaces [24]. As such, note that, although the simulated annealing durations are extremely small as compared to those reached experimentally, the simulated systems also feature a much smaller surface and, as such, exchange heat significantly faster with the thermostat. Altogether, as shown below, the simulated annealing used herein yields variations of density that are comparable to those observed experimentally, which allows us to make qualitative comparisons between the experimental and simulation results presented herein.

2.4. Simulations of fracture

The influence of the temperature and pressure histories on the mode I fracture (i.e., under a tensile stress orthogonal to the plane in which the crack propagates) of the studied glasses was then simulated by MD. To compute fracture toughness, we relied on the energetic approach of fracture mechanics [25–27]. We first manually inserted a sharp initial crack in the (x, y) plane. After a relaxation to zero pressure, the system was elongated step-wise in the direction z by small increments (1%) of tensile strain. During each step, the system was relaxed for 50 ps, followed by another 50 ps for statistical averaging of the properties. Note that we examined the effect of the strain rate and found that, provided it is sufficiently low (< 0.5 ns^{-1}), no significant influence on the obtained stress–strain curve is observed. Once the system is broken, the stress goes back to zero, so that the fracture energy G_c can be estimated by integrating the stress over the strain. The relationship between K_c and G_c is then given by the Irwin formula [28]. This methodology, whose details can be found in Refs. [9,29–31], was shown to offer realistic values of fracture toughness for various silicate glasses [9]. In complement, the surface energy γ_s of the glasses was roughly estimated by cutting the system into two parts, letting it relax for 25 ps, and computing the resulting change of the potential energy of the system (see Ref. [30]).

3. Results

3.1. Glass density

The influence of the temperature and pressure histories on the density of the experimental and simulated glasses is shown in **Fig. 1** (more details can be found in Ref. [21]). Overall, we note that density increases, both upon annealing and quenching under pressure. Such a behavior arises from the facts that, upon annealing, the fictive temperature of the glass decreases, which results in more compact atomic networks [32], whereas, upon quenching under pressure, the glass undergoes inelastic densification, that is, it remains partially densified at ambient pressure once at room temperature. Considering the annealing time and pressures used herein, we

observe that pressure quenching results in larger variations of density than annealing. Further, we note that, despite having different compositions and synthesis protocols, the experimental and simulated glasses show variations of density that are in agreement with each other – in terms of both magnitude and trend. This supports the fact that experimental and simulation outcomes can be meaningfully compared herein. Altogether, we observe that the temperature and pressure histories show distinct effects on the compactness of the atomic network [21]. As such, these systems can be used to assess whether composition and density fully determine the fracture toughness of glasses, or if it further depends on the details of the temperature and pressure histories.

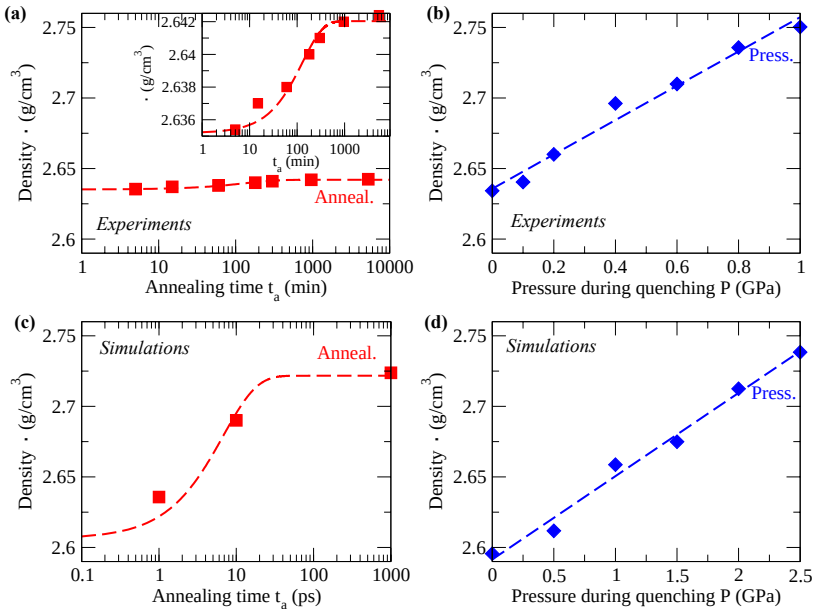

Fig. 1. *Variation of density at ambient temperature and pressure induced by (a, c) thermal annealing and (b, d) quenching under pressure, as obtained from experiments and simulations, respectively [21]. Lines serve as guides for the eye. The inset shows a zoom on the data presented on the panel (a) for improved visibility.*

3.2. Fracture toughness

The density dependence of indentation fracture toughness of the samples is shown in **Fig. 2**a. We first observe that annealing and quenching under pressure both result in a decrease of K_c. This is in agreement with previous observations for various compositions of glasses [17,33–35], and has been attributed to the fact that, upon indentation, pre-densified glasses show a lower ability to permanently densify with respect to shear flow deformations [33,36]. The partial loss of permanent densification, a mechanism through which stress can be relaxed at the vicinity of the indenter tip, results in increased values of hardness [21], but, in turn, promotes crack initiation and growth, thereby resulting in lower values of fracture toughness [33]. Further, we note that, at a given glass density, the loss of K_c resulting from annealing is significantly larger than that induced by quenching under pressure. As shown in **Fig. 2**b, the simulated glasses show a similar behavior. Indeed, although the absolute value of the computed fracture

toughness differs from that obtained experimentally – which might be due to the differing glass compositions or the uncertainty arising from the use of Vickers indentation – the simulated annealing also results in a decrease of fracture toughness that is larger than that induced by quenching under pressure, at a given density. Once again, this demonstrates the ability of the simulations conducted herein to offer a realistic description of annealing and pressure effects on glass fracture. Overall, these results demonstrate that, for a given composition, density does not fully control macroscopic properties like fracture toughness, which, in turn, appears to strongly depend on the details of the temperature and pressure histories of the glass. Note that similar conclusions apply to hardness [21].

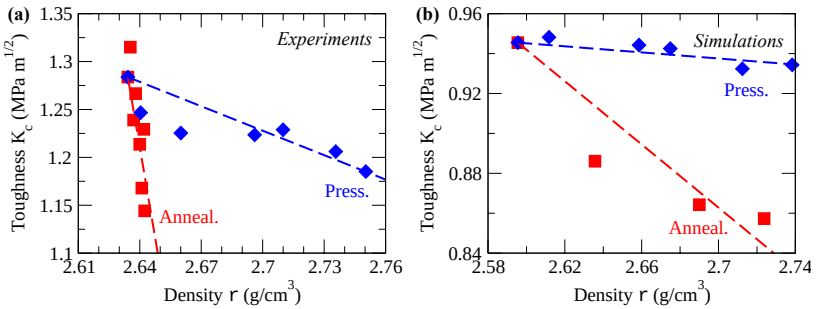

Fig. 2. *Variation of fracture toughness induced by thermal annealing and quenching under pressure with respect to density, as obtained from (a) indentation experiments and (b) MD simulations. Lines serve as guides for the eye.*

4. Discussion

We now investigate the mechanical and structural origins of the differing roles of temperature and pressure histories on fracture toughness. To this end, since they have been shown to offer a realistic description of the glass studied herein, we used our atomistic simulations to access mechanistic and structural details that would be challenging to obtain experimentally. First, we assess the degree of brittleness of the fracture by computing the different contributions to the fracture energy G_c. G_c is related to the surface energy γ_s by:

$$G_c = 2\gamma_s + G_{diss} \qquad \text{(Eq. 1)}$$

where G_{diss} captures all forms of dissipated energy. A brittleness index B can then be introduced as:

$$B = 2\gamma_s / G_c \qquad \text{(Eq. 2)}$$

wherein B would be equal to 1 for a perfectly brittle material. As such, this formalism provides a direct and non-arbitrary fashion to characterize the degree of brittleness of fracture.

The evolution of the surface energy with density is shown in **Fig. 3**a. We note that, in contrast to the fracture toughness, γ_s increases with density. This trend is in agreement with previous

observations [31] and can be understood from the fact that higher density results in the existence of more bonds per unit of surface. As such, the formation of a surface from a bulk glass requires to break more bonds and, hence, costs a higher amount of energy, thereby resulting in higher values of γ_s. We then note that, at constant density, γ_s increases slightly more upon annealing than quenching under pressure. As detailed in Ref. [21], this may arise from the fact that annealing results in the strengthening of angular bonds, thereby enhancing the energy needed to break them, whereas they remain largely unaffected after quenching under pressure.

The knowledge of G_c and γ_s allows us to evaluate the brittleness index B, which is shown in **Fig. 3**b. We first note that, although aluminosilicate glasses typically exhibit brittle fracture at the macroscopic scale, we find here that B is systematically lower than 1, that is, upon crack propagation, a significant portion of the fracture energy is dissipated rather than being used to create new surfaces. This suggests that, although brittle at the macroscale, glasses can break in a ductile way at the nanoscale. The existence of such nano-ductility is in agreement with experiments [8,37] and simulations [9,38] and has recently been shown to be intrinsic to multi-component glasses [10]. We then observe that B increases with density, both upon annealing and quenching under pressure. This is in agreement with previous results on densified sodium silicate glasses, for which a ductile-to-brittle transition induced by pressure was observed [31]. As mentioned above, this is likely partially due to the fact that pre-densified glasses lose the ability to dissipate energy through plastic densification [33]. We also note that annealing, by inducing a sharpening of the radial and angular bond distributions [21], results in an overall loss of topological heterogeneity in the network. As such, the fact that such heterogeneity has been found to increase nanoductility is consistent with the present findings [10]. Eventually, we observe that brittleness increases significantly more upon annealing than quenching under pressure. This demonstrates that, at fixed composition, glass brittleness is not only controlled by density, i.e., by the amount of free volume. In other terms, the presence or not of free volume in the atomic network and, as such, the potential propensity for densification, is not the only contribution to glass brittleness. Finally, as shown in **Fig. 3**c, it is worth noting that the brittleness index B shows a trend that is qualitatively similar to that of the crack-to-indent ratio (c/a), which supports the fact that the latter metric can be used as an indicator of the degree of brittleness [39]. Overall, these results show that the decrease of fracture toughness typically observed in densified glasses does not arise from a loss of cohesion (as captured by γ_s), but rather from an enhancement of brittleness.

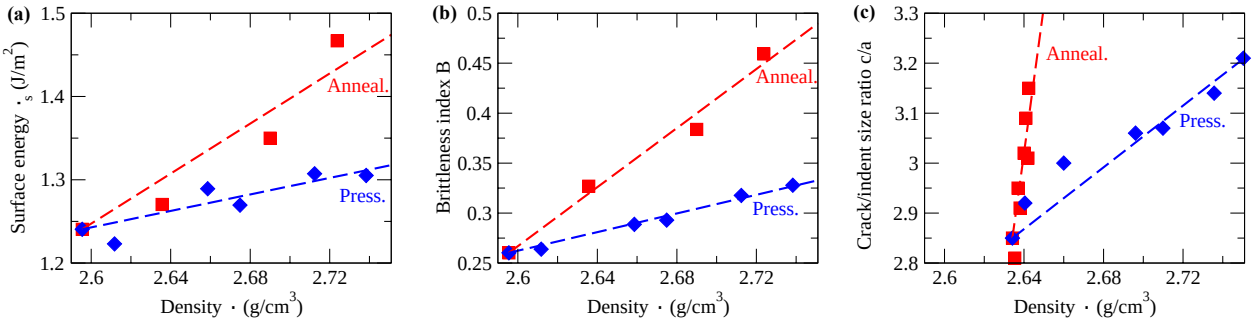

Fig. 3. *Computed (a) surface energy and (b) brittleness index (see Eq. 2) with respect to density, as obtained after thermal annealing and quenching under pressure. (c) Measured ratio of crack length to half diagonal of the indent (c/a) for an applied indentation load of 9.8 N. Lines serve as guides for the eye.*

Finally, we utilize the outcomes of the simulations to seek for a structural origin of the enhancement of brittleness observed herein. Note that a complete analysis of the structural effects of annealing and quenching under pressure is available in Ref. [21], so that only the most relevant features are provided herein. First, as detailed in Ref. [21], it is reminded that the increase of density experienced upon quenching under pressure primarily arises from a medium-range compaction, as evidenced by a shift of the first sharp diffraction peak of the structure factor towards higher values of reciprocal wavelengths *Q*. On the other hand, short-range order structural features (bond lengths, angles, coordination numbers) remain largely unaffected. As such, the moderate enhancement of brittleness induced by quenching under pressure appears to purely arise from a loss of available free volume at the medium-range order.

On the other hand, annealing has only little effect on the medium-range order. In contrast with pressure, the increase of density induced by annealing mainly involves variations in the short-range order and, in particular, in the Si–O–Si bond angle distribution (BAD) [21]. This is illustrated by **Fig. 4**a and b, which show the average value and standard deviation of the Si–O–Si BAD, respectively. We first note that annealing results in a significant increase of the average value of the Si–O–Si BAD, whereas the BAD remains largely unaffected by pressure. This is in agreement with recent MD results showing that, as the cooling rate decreases, that is, as the glass relaxes to lower energy states, the Si–O–Si BAD of silica shifts towards higher angles [40]. We then observe that the standard deviation of the Si–O–Si BAD, which represents the angular excursion between Si tetrahedra, decreases upon annealing, whereas, once again, it is only weakly affected by pressure. This trend, which is in agreement with the loss of inter-tetrahedral rigid unit modes observed in densified silica [41,42], is also observed for the Al–O–Al and Si–O–Al BADs.

These results suggest that the relative motion between Si or Al tetrahedra, which is greatly inhibited upon annealing, drives the enhancement of brittleness. In fact, as shown in **Fig. 4**c, the fracture toughness linearly increases with the extent of the inter-tetrahedral angular excursion, independently of the densification method – although we note that the glasses

quenched under pressure slightly deviate from this trend, which suggests that the medium range order can also weakly affect fracture toughness, as a second order parameter. Overall, this clearly establishes that the inter-tetrahedral relative motion plays a primary role in controlling fracture toughness and nano-ductility, and suggests the following atomistic picture. As SiO_4 and AlO_4 tetrahedra are mostly rigid units, the atomic networks of silicate glasses subjected to stress can only reorganize through relative reorganizations between the tetrahedra. As the inter-tetrahedral angle becomes more rigid, the propensity for such nano-ductile modes of stress relaxation is reduced, which renders the glass more brittle and, thereby, less tough. Note that the extent of inter-tetrahedral angular motion also appears to play a critical role in impacting glass properties such as hardness [43] or glass forming ability [44,45].

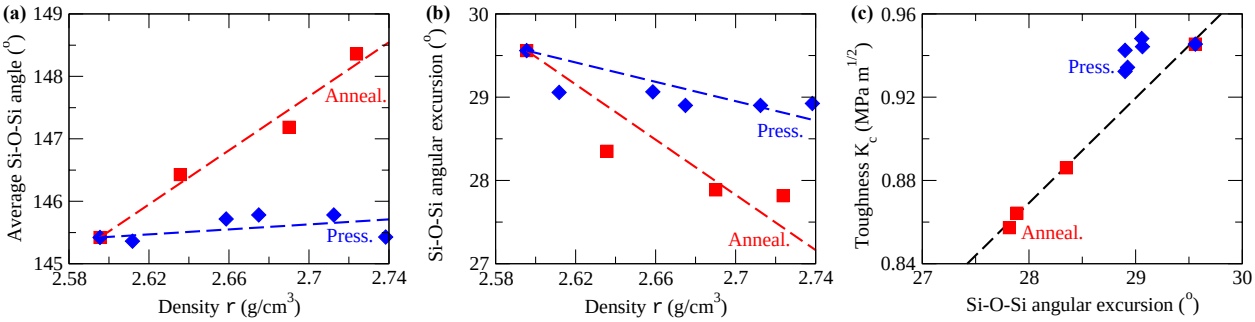

Fig. 4. *Computed (a) average value and (b) broadness (2σ) of the Si–O–Si bond angle distribution with respect to density, as obtained after thermal annealing and quenching under pressure [21]. (c) Fracture toughness as a function of 2σ. Lines serve as guides for the eye.*

5. Conclusions

Overall, these results highlight that density alone is not a good order parameter for glass mechanical properties, which, in turn, are influenced by temperature and pressure histories. Interestingly, annealing and quenching under pressure allows one to isolate the effect of structure only, i.e., at fixed composition, and, as such, can offer new insights into structure-properties relationships in glasses. Specifically, this study demonstrates that, at fixed composition, fracture toughness is strongly affected by variations in the short-range order, but only weakly depends on the details on the medium-range order. Such short-range features can be conveniently captured by topological constraint theory [46,47], which strongly calls for a topological description of fracture toughness [31].

Acknowledgements

This work was partially funded by Corning Incorporated and the National Science Foundation under Grant No. 1562066. M. M. S. acknowledges financial support from the Danish Council for Independent Research under Sapere Aude: DFF-Starting Grant (1335-00051A). S. J. R. acknowledges financial support from the National Science Center of Poland under Grant No. UMO-2011/03/B/ST3/02352.

References

[1] P. Ball, Material witness: Concrete mixing for gorillas, Nat Mater. 14 (2015) 472–472. doi:10.1038/nmat4279.

[2] J.C. Mauro, A.J. Ellison, L.D. Pye, Glass: The Nanotechnology Connection, International Journal of Applied Glass Science. 4 (2013) 64–75. doi:10.1111/ijag.12030.

[3] J.C. Mauro, M.M. Smedskjaer, Unified physics of stretched exponential relaxation and Weibull fracture statistics, Physica A: Statistical Mechanics and Its Applications. 391 (2012) 6121–6127. doi:10.1016/j.physa.2012.07.013.

[4] L. Wondraczek, J.C. Mauro, J. Eckert, U. Kühn, J. Horbach, J. Deubener, T. Rouxel, Towards Ultrastrong Glasses, Adv. Mater. 23 (2011) 4578–4586. doi:10.1002/adma.201102795.

[5] D.C. Hofmann, J.-Y. Suh, A. Wiest, G. Duan, M.-L. Lind, M.D. Demetriou, W.L. Johnson, Designing metallic glass matrix composites with high toughness and tensile ductility, Nature. 451 (2008) 1085–1089. doi:10.1038/nature06598.

[6] M. Mirkhalaf, A.K. Dastjerdi, F. Barthelat, Overcoming the brittleness of glass through bio-inspiration and micro-architecture, Nat Commun. 5 (2014). doi:10.1038/ncomms4166.

[7] O.S. Narayanaswamy, Stress and Structural Relaxation in Tempering Glass, Journal of the American Ceramic Society. 61 (1978) 146–152. doi:10.1111/j.1151-2916.1978.tb09259.x.

[8] F. Celarie, S. Prades, D. Bonamy, L. Ferrero, E. Bouchaud, C. Guillot, C. Marlière, Glass Breaks like Metal, but at the Nanometer Scale, Phys. Rev. Lett. 90 (2003) 075504. doi:10.1103/PhysRevLett.90.075504.

[9] B. Wang, Y. Yu, Y.J. Lee, M. Bauchy, Intrinsic Nano-Ductility of Glasses: The Critical Role of Composition, Front. Mater. 2 (2015) 11. doi:10.3389/fmats.2015.00011.

[10] B. Wang, Y. Yu, M. Wang, J.C. Mauro, M. Bauchy, Nanoductility in silicate glasses is driven by topological heterogeneity, Phys. Rev. B. 93 (2016) 064202. doi:10.1103/PhysRevB.93.064202.

[11] J.C. Mauro, C.S. Philip, D.J. Vaughn, M.S. Pambianchi, Glass Science in the United States: Current Status and Future Directions, Int J Appl Glass Sci. 5 (2014) 2–15. doi:10.1111/ijag.12058.

[12] J.C. Mauro, E.D. Zanotto, Two Centuries of Glass Research: Historical Trends, Current Status, and Grand Challenges for the Future, Int J Appl Glass Sci. 5 (2014) 313–327. doi:10.1111/ijag.12087.

[13] J.C. Mauro, Grand challenges in glass science, Front. Mater. 1 (2014) 20. doi:10.3389/fmats.2014.00020.

[14] P.S. Danielson, A.J.G. Ellison, N. Venkataraman, Glass compositions having high thermal and chemical stability and methods of making thereof, US7833919 B2, 2010. http://www.google.com/patents/US7833919 (accessed August 7, 2016).

[15] S. Bhosle, K. Gunasekera, P. Boolchand, M. Micoulaut, Melt Homogenization and Self-Organization in Chalcogenides-Part I, Int J Appl Glass Sci. 3 (2012) 189–204. doi:10.1111/j.2041-1294.2012.00093.x.

[16] M.M. Smedskjaer, S.J. Rzoska, M. Bockowski, J.C. Mauro, Mixed alkaline earth effect in the compressibility of aluminosilicate glasses, The Journal of Chemical Physics. 140 (2014) 054511. doi:10.1063/1.4863998.

[17] S. Striepe, M.M. Smedskjaer, J. Deubener, U. Bauer, H. Behrens, M. Potuzak, R.E. Youngman, J.C. Mauro, Y. Yue, Elastic and micromechanical properties of isostatically

compressed soda–lime–borate glasses, Journal of Non-Crystalline Solids. 364 (2013) 44–52. doi:10.1016/j.jnoncrysol.2013.01.009.
[18] K. Niihara, R. Morena, D.P.H. Hasselman, Evaluation ofKIc of brittle solids by the indentation method with low crack-to-indent ratios, J Mater Sci Lett. 1 (n.d.) 13–16. doi:10.1007/BF00724706.
[19] B.R. Lawn, D.B. Marshall, Hardness, Toughness, and Brittleness: An Indentation Analysis, Journal of the American Ceramic Society. 62 (1979) 347–350. doi:10.1111/j.1151-2916.1979.tb19075.x.
[20] G.D. Quinn, R.C. Bradt, On the Vickers Indentation Fracture Toughness Test, Journal of the American Ceramic Society. 90 (2007) 673–680. doi:10.1111/j.1551-2916.2006.01482.x.
[21] M.M. Smedskjaer, M. Bauchy, J.C. Mauro, S.J. Rzoska, M. Bockowski, Unique effects of thermal and pressure histories on glass hardness: Structural and topological origin, The Journal of Chemical Physics. 143 (2015) 164505. doi:10.1063/1.4934540.
[22] M. Bouhadja, N. Jakse, A. Pasturel, Structural and dynamic properties of calcium aluminosilicate melts: A molecular dynamics study, The Journal of Chemical Physics. 138 (2013) 224510. doi:10.1063/1.4809523.
[23] M. Bauchy, Structural, vibrational, and elastic properties of a calcium aluminosilicate glass from molecular dynamics simulations: The role of the potential, The Journal of Chemical Physics. 141 (2014) 024507. doi:10.1063/1.4886421.
[24] Y. Guissani, B. Guillot, A computer simulation study of the liquid–vapor coexistence curve of water, The Journal of Chemical Physics. 98 (1993) 8221. doi:doi:10.1063/1.464527.
[25] A.A. Griffith, The phenomena of rupture and flow in solids, Philosophical Transactions of the Royal Society of London. Series A, Containing Papers of a Mathematical or Physical Character. 221 (1921) 163–198.
[26] J.-B. Leblond, Mecanique de la rupture fragile et ductile, Lavoisier, Lavoisier, Paris, 2003.
[27] T.L. Anderson, Fracture mechanics: fundamentals and applications, CRC PressI Llc, 2005.
[28] G.R. Irwin, Fracture in “Handbuch der Physik,” vol. V, New York, NY: Springer, 1958.
[29] Y. Yu, B. Wang, Y.J. Lee, M. Bauchy, Fracture Toughness of Silicate Glasses: Insights from Molecular Dynamics Simulations, in: Symposium UU – Structure-Property Relations in Amorphous Solids, 2015. doi:10.1557/opl.2015.50.
[30] M. Bauchy, H. Laubie, M.J. Abdolhosseini Qomi, C.G. Hoover, F.-J. Ulm, R.J.-M. Pellenq, Fracture toughness of calcium–silicate–hydrate from molecular dynamics simulations, Journal of Non-Crystalline Solids. 419 (2015) 58–64. doi:10.1016/j.jnoncrysol.2015.03.031.
[31] M. Bauchy, M.J.A. Qomi, C. Bichara, F.-J. Ulm, R.J.-M. Pellenq, Topological Origin of Fracture Toughening in Complex Solids: the Viewpoint of Rigidity Theory, arXiv:1410.2916 [cond-Mat]. (2014). http://arxiv.org/abs/1410.2916 (accessed December 10, 2014).
[32] A.K. Varshneya, Fundamentals of Inorganic Glasses, Academic Press Inc, 1993.
[33] K.G. Aakermann, K. Januchta, J.A.L. Pedersen, M.N. Svenson, S.J. Rzoska, M. Bockowski, J.C. Mauro, M. Guerette, L. Huang, M.M. Smedskjaer, Indentation deformation mechanism of isostatically compressed mixed alkali aluminosilicate glasses, Journal of Non-Crystalline Solids. 426 (2015) 175–183. doi:10.1016/j.jnoncrysol.2015.06.028.
[34] M.N. Svenson, T.K. Bechgaard, S.D. Fuglsang, R.H. Pedersen, A.Ø. Tjell, M.B. Østergaard, R.E. Youngman, J.C. Mauro, S.J. Rzoska, M. Bockowski, M.M. Smedskjaer, Composition-

Structure-Property Relations of Compressed Borosilicate Glasses, Phys. Rev. Applied. 2 (2014) 024006. doi:10.1103/PhysRevApplied.2.024006.
[35] Z. Zhang, N. Soga, K. Hirao, Indentation deformation and fracture of densified silicate glass, Journal of Materials Science. 30 (1995) 6359–6362. doi:10.1007/BF00369689.
[36] S. Striepe, J. Deubener, M. Potuzak, M.M. Smedskjaer, A. Matthias, Thermal history dependence of indentation induced densification in an aluminosilicate glass, Journal of Non-Crystalline Solids. 445–446 (2016) 34–39. doi:10.1016/j.jnoncrysol.2016.04.046.
[37] A. Livne, E. Bouchbinder, J. Fineberg, Breakdown of Linear Elastic Fracture Mechanics near the Tip of a Rapid Crack, Phys. Rev. Lett. 101 (2008) 264301. doi:10.1103/PhysRevLett.101.264301.
[38] Y.-C. Chen, Z. Lu, K. Nomura, W. Wang, R.K. Kalia, A. Nakano, P. Vashishta, Interaction of Voids and Nanoductility in Silica Glass, Phys. Rev. Lett. 99 (2007) 155506. doi:10.1103/PhysRevLett.99.155506.
[39] J. Sehgal, S. Ito, A New Low-Brittleness Glass in the Soda-Lime-Silica Glass Family, Journal of the American Ceramic Society. 81 (1998) 2485–2488. doi:10.1111/j.1151-2916.1998.tb02649.x.
[40] J.M.D. Lane, Cooling rate and stress relaxation in silica melts and glasses via microsecond molecular dynamics, Phys. Rev. E. 92 (2015) 012320. doi:10.1103/PhysRevE.92.012320.
[41] K. Trachenko, M.T. Dove, Intermediate state in pressurized silica glass: Reversibility window analogue, Phys. Rev. B. 67 (2003). doi:10.1103/PhysRevB.67.212203.
[42] K. Trachenko, M.T. Dove, V. Brazhkin, F.S. El'kin, Network rigidity and properties of SiO_2 and GeO_2 glasses under pressure, Phys. Rev. Lett. 93 (2004). doi:10.1103/PhysRevLett.93.135502.
[43] M. Bauchy, M.J.A. Qomi, C. Bichara, F.-J. Ulm, R.J.-M. Pellenq, Rigidity Transition in Materials: Hardness is Driven by Weak Atomic Constraints, Phys. Rev. Lett. 114 (2015) 125502. doi:10.1103/PhysRevLett.114.125502.
[44] M. Zhang, P. Boolchand, The Central Role of Broken Bond-Bending Constraints in Promoting Glass Formation in the Oxides, Science. 266 (1994) 1355–1357. doi:10.1126/science.266.5189.1355.
[45] M. Bauchy, M. Micoulaut, M. Celino, S. Le Roux, M. Boero, C. Massobrio, Angular rigidity in tetrahedral network glasses with changing composition, Phys. Rev. B. 84 (2011) 054201. doi:10.1103/PhysRevB.84.054201.
[46] J.C. Mauro, Topological constraint theory of glass, Am. Ceram. Soc. Bull. 90 (2011) 31–37.
[47] M. Bauchy, Topological constraints and rigidity of network glasses from molecular dynamics simulations, American Ceramic Society Bulletin. 91 (2012) 34–38A.

Figure

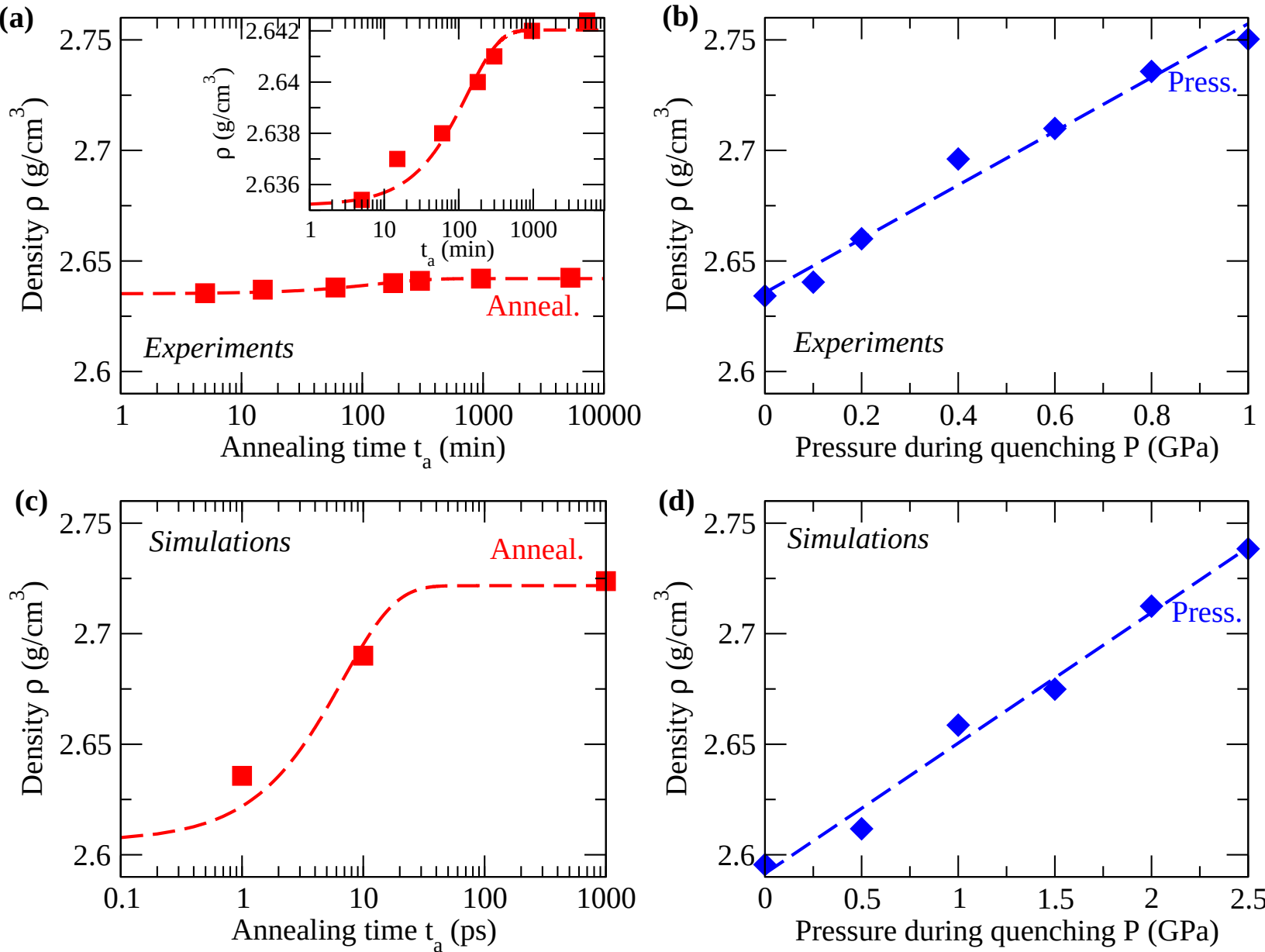
(a)
Density ρ (g/cm^3)
2.75
2.7
2.65
2.6
1
10
100
1000
10000
Annealing time t$_a$ (min)
Anneal.
Experiments
ρ (g/cm^3)
2.642
2.64
2.638
2.636
1
10
100
1000
t$_a$ (min)
(b)
Density ρ (g/cm^3)
2.75
2.7
2.65
2.6
0
0.2
0.4
0.6
0.8
1
Pressure during quenching P (GPa)
Press.
Experiments
(c)
Density ρ (g/cm^3)
2.75
2.7
2.65
2.6
0.1
1
10
100
1000
Annealing time t$_a$ (ps)
Simulations
Anneal.
(d)
Density ρ (g/cm^3)
2.75
2.7
2.65
2.6
0
0.5
1
1.5
2
2.5
Pressure during quenching P (GPa)
Simulations
Press.

Figure

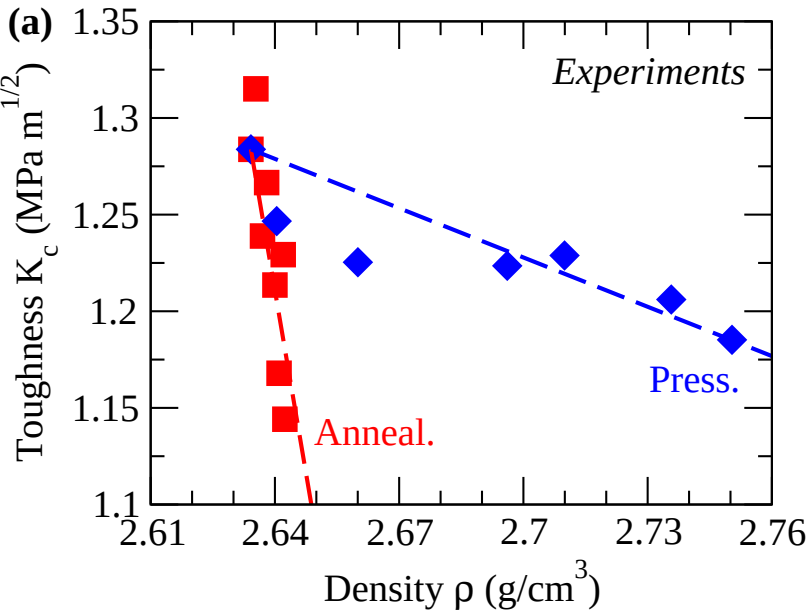
(a)
Experiments
Press.
Anneal.
Toughness K_c (MPa $m^{1/2}$)
Density ρ (g/cm^3)
1.35
1.3
1.25
1.2
1.15
1.1
2.61
2.64
2.67
2.7
2.73
2.76

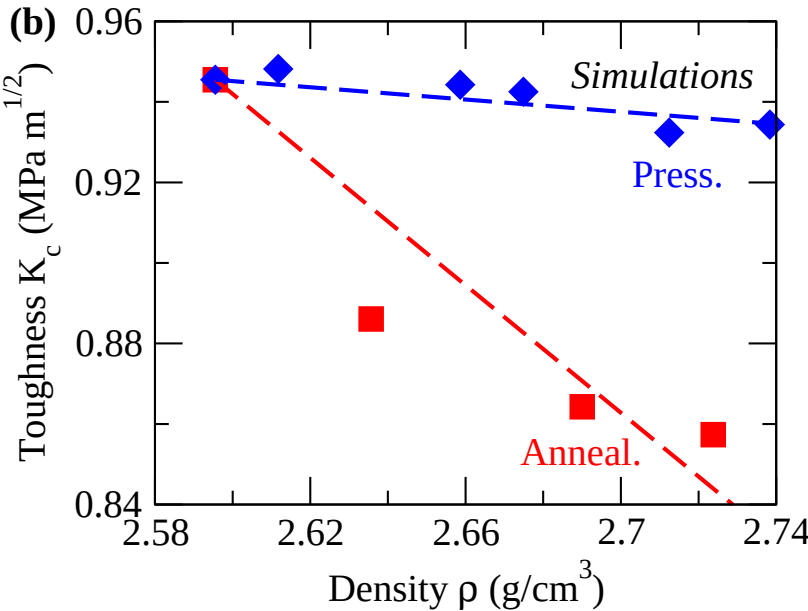
(b)
Simulations
Press.
Anneal.
Toughness K_c (MPa $m^{1/2}$)
Density ρ (g/cm^3)
0.96
0.92
0.88
0.84
2.58
2.62
2.66
2.7
2.74

Figure

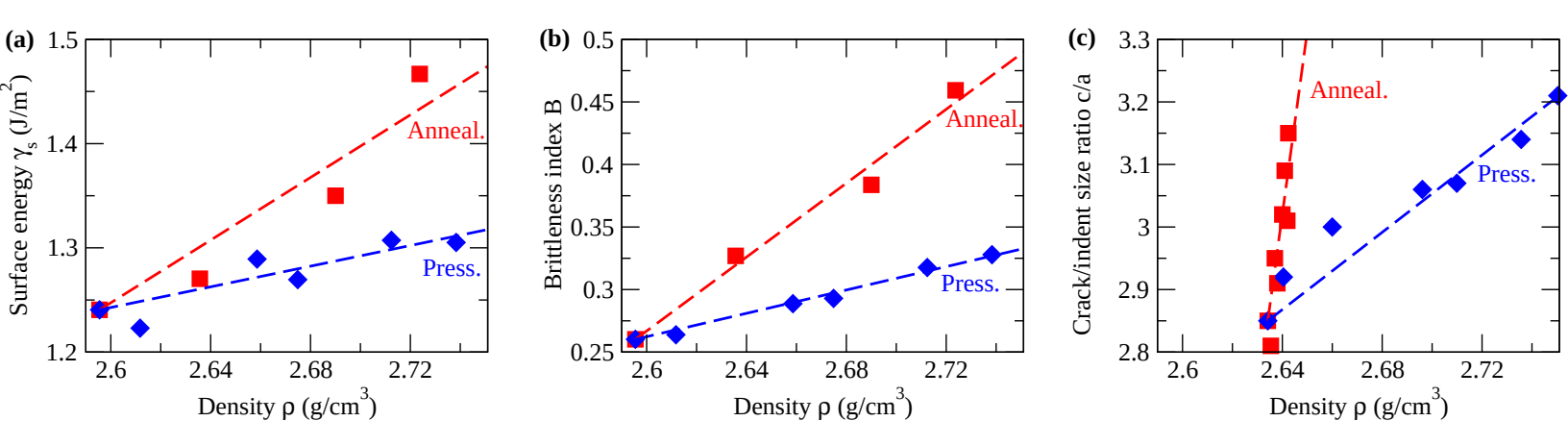
(a)
Surface energy γ_s (J/m^2)
1.5
1.4
1.3
1.2
2.6
2.64
2.68
2.72
Density ρ (g/cm^3)
Anneal.
Press.
(b)
Brittleness index B
0.5
0.45
0.4
0.35
0.3
0.25
2.6
2.64
2.68
2.72
Density ρ (g/cm^3)
Anneal.
Press.
(c)
Crack/indent size ratio c/a
3.3
3.2
3.1
3
2.9
2.8
2.6
2.64
2.68
2.72
Density ρ (g/cm^3)
Anneal.
Press.

Figure

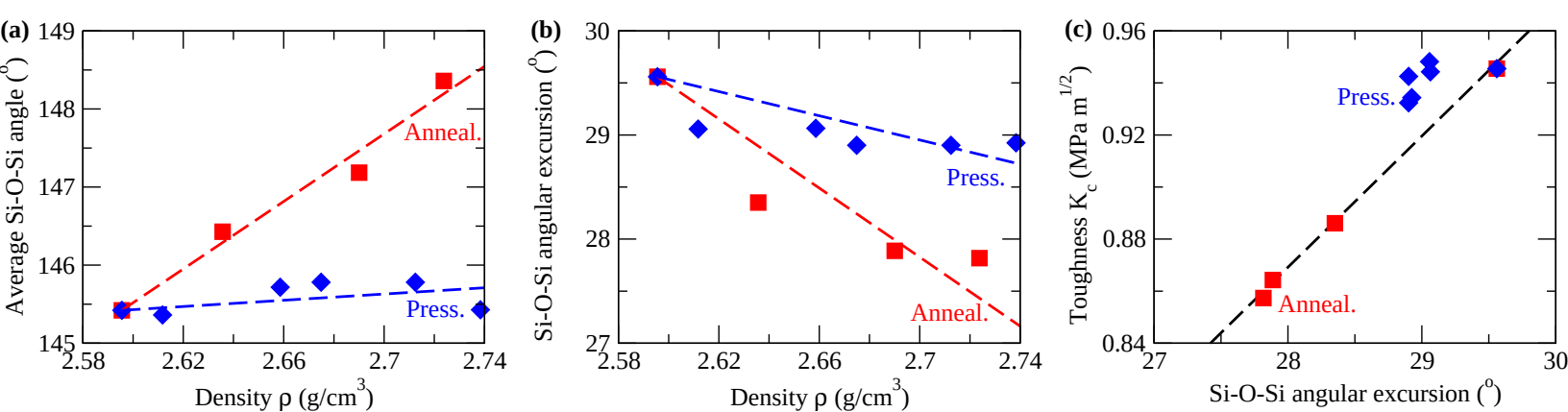
(a)
Average Si-O-Si angle (°)
149
148
147
146
145
2.58
2.62
2.66
2.7
2.74
Density ρ (g/cm3)
Anneal.
Press.
(b)
Si-O-Si angular excursion (°)
30
29
28
27
2.58
2.62
2.66
2.7
2.74
Density ρ (g/cm3)
Press.
Anneal.
(c)
Toughness Kc (MPa m1/2)
0.96
0.92
0.88
0.84
27
28
29
30
Si-O-Si angular excursion (°)
Press.
Anneal.